IGARSS 2021 - 2021 IEEE International Geoscience and Remote Sensing Symposium | 978-1-6654-0369-6/21/$31.00 ©2021 IEEE | DOI: 10.1109/IGARSS47720.2021.9553716

FORMATION-FLYING SAR RECEIVERS IN FAR-FROM-TRANSMITTER GEOMETRY: X-BAND SAR ANTENNA DESIGN

Gerardo Di Martino, Alessio Di Simone, Michele Grassi, Marco Grasso, Maria Daniela Graziano, Antonio Iodice, Antonio Moccia, Alfredo Renga, Daniele Riccio, Giuseppe Ruello

Università degli Studi di Napoli Federico II, Napoli, Italy

ABSTRACT

This paper discusses a new receiving antenna for remote sensing applications to be mounted onboard a formation-flying synthetic aperture radar (FF-SAR) bistatic system based on the CubeSat standard. The formation works as a bistatic SAR collecting microwave signals coming from a transmitting SAR unit. The receiving antenna has been designed according to the acquisition modes of the formation, namely a stripmap mode for signal-to-noise ratio improvement and a High-Resolution Wide-Swath mode for the monitoring of large regions. In order to meet the very different requirements for both operating modes with the physical constraints imposed by the nanosat geometry, a large reflector with reconfigurable feed has been conceived and simulated. The results show that the proposed antenna accomplishes the design specifications.

***Index Terms*—** reflector antennas, antenna feed, bistatic SAR, formation-flying SAR, nano-satellites.

1. INTRODUCTION

In the last decade, growing interest in science missions based on nano-satellites and, in particular, CubeSats has exploded. As a matter of fact, the number of nano-satellites placed into orbit every year keeps increasing and almost one-thousand nanosat missions have been launched in the past five years [1]. Light-weight, compactness, low cost, modularity, and COTS-based system components, have made the CubeSat standard the new frontier for space-based Earth observation and remote sensing. Among CubeSat systems, formation-flying synthetic aperture radar (FF-SAR) enables new acquisition modes by coherently processing in a proper way the signals emitted by a transmitter and scattered off the illuminated scene.

In this paper, we present the design of the receiving X-band SAR antenna for a FF-SAR based on a fleet of three 12U CubeSat platforms. The antenna is conceived for two operational modes, namely signal-to-noise ratio (SNR) improvement and high-resolution wide-swath (HRWS) imaging. A more detailed description of the signal processing scheme is provided in the companion paper [2].

2. FF-SAR ACQUISITION MODES

The investigated system combines the advantages of a sensor distributed onboard different CubeSats with those of a bistatic radar working with an illuminator of opportunity. Since the transmitter is a monostatic SAR, it is possible to combine monostatic and bistatic data reflected by common covered areas [3]. From the point of view of the applications the formation of passive receivers can be considered as a single high performance bistatic receiver enabling applications that are not possible by monostatic missions. However, differently from a larger monolithic system, the cluster is scalable, meaning the imaging performance is in direct relation to the number and spacing of receivers. Indeed, as an FF-SAR [4], the distributed payload drastically improves the flexibility, reliability and modularity of the overall system when compared to a much larger monolithic one. Moreover, single members of the system can be replaced in case of failure, thus guaranteeing graceful performance degradation and preserving mission goals.

Most of past mission concepts dealing with multi satellite missions were focused on the operation of a multi-baseline single-pass interferometer. Such a configuration has been proposed for digital elevation model generation, to implement advanced InSAR techniques like single-pass tomography and Ground Moving Target Indication (GMTI) or to complement the processing architectures of DInSAR through repeated multi-baseline single-pass acquisitions. Those concepts only exploited the combination of more images for interferometric applications thus asking for natively higher performance images, hence requiring larger platforms. The present system follows a completely different approach. The high performance image synthesized by the cluster of CubeSats guarantees enhanced properties with respect to the image that a single receiver of the formation can generate when operating as an independent unit: this relaxes the requirements which apply to each receiver thus enabling the realization through CubeSats.

The system is conceived to apply two different acquisition modes (AMs), namely:

– AM1 – SNR improvement, in which the signals gathered by each member of the cluster are properly processed to improve the SNR of the combined signal.
– AM2 – HRWS imaging, in which the signals received by each CubeSat is properly handled to enable high resolution over the large observed swath.

The rationale behind AM1 and AM2 is discussed in [2].

3. ANTENNA DESIGN

The bistatic geometry shown in Figure 1 has been considered for the design of the receiving SAR antenna. Parameters of the geometry are listed in Table I. In particular, it is assumed that the receiving satellites are in the same orbit of the transmitter, which is a pre-existing SAR system of opportunity operating at X-band, e.g., COSMO-SKyMed or PLATiNO-1 [5]. In addition, according to [2], it is assumed that a minimum swath range of 15 km is required in AM1, whereas in AM2 the receiving antenna should collect the transmitted SAR signal coming from a region as large as 100 km in the range direction.
Given the bistatic geometry in Figure 1, such requirements lead to the minimum half-power beamwidth (HPBW) values reported in Table II, which also includes other requirements to be fulfilled by the receiving SAR antenna module. In particular, the minimum required gain of 34.8 dBi in AM1 ensures that a formation of at least three satellites offers better performance in terms of noise equivalent sigma zero (NESZ) with respect to a monostatic SAR system.

From Table II it emerges that contrasting features are required in the two AMs. Indeed, an adequate improvement of the SNR calls for a high-gain antenna in AM1, whereas a sufficiently large HPBW is required for ensuring wide range swaths in AM2. Additionally, the strict constraints on volume and mass imposed by the CubeSat standard make impractical the installation of two different antennas, each optimized for an AM. The solution we propose here is based on a parabolic reflector large enough to meet the high-gain requirement in AM1. The large HPBW needed in AM2 is then obtained through a reconfigurable feed based on a patch array.

Table I: Parameters of the bistatic configuration

Symbol	Parameter	Value
d_{RxTx}	Along-track baseline	100 km
h_{Rx}	Rx height	410 km
h_{Tx}	Tx height	410 km
L_A	Tx antenna size (azimuth)	3.4 m
L_R	Tx antenna size (range)	0.7 m
ϑ	Looking angle	20 – 40 deg
S_r	Range swath	15 km (AM1) Up to 100 km (AM2)
S_a	Azimuth footprint	5 km

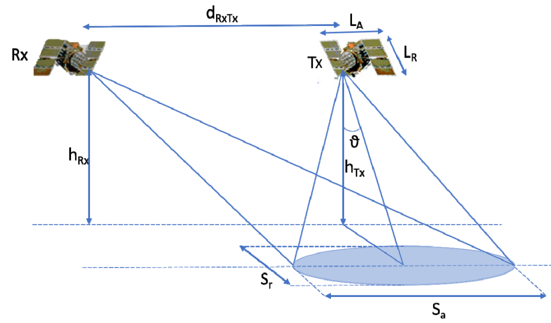

Figure 1: Bistatic geometry of the FF-SAR. The transmitter is a side-looking SAR, while the receiving units are properly squinted to cover the region illuminated by the transmitter.

Table II: Antenna requirements

Parameter	Value
Volume	≤ 3U
Mass	≤ 3.2 kg
Frequency	9.6 GHz – X-band
Pointing	20 – 40 deg
Signal bandwidth	≥ 80 MHz
Gain	> 34.8 dBi (AM1 with N_{sat} = 3)
HPBW range	≥ 1.79 deg in AM1 ≥ 11.1 deg in AM2
HPBW azimuth	≥ 0.61 deg

The geometry of the reflector and of the feed are shown in Figure 2(a) and Figure 2(b), respectively. The KaTENNa parabolic reflector was selected as the reflecting dish thanks to its high-gain performance and suitability with 12U CubeSat class. More specifically, the radius R and the focal length L_f of the parabolic dish are set to 0.5 m and 0.75 m, respectively. Such choices lead to a tapering angle α_a equal to 36.9° and to L_h equal to 0.083 m. Such values are suitable with a 3U stowage and with an umbrella-like deployment mechanism [6].

The feed is a 2x12 patch array, whose elements are properly connected to the receiver according to the acquisition mode. An inter-element spacing of λ/2 ensures the absence of grating lobes which would negatively affect the radiation pattern of the reflector and, at the same time, maximizes the feed aperture. The dielectric substrate separating the patches from the ground plane is designed with Rogers RO4003C material which exhibits a dielectric constant of 3.55 and a loss tangent of 0.0027 at 10 GHz. This substrate has been successfully adopted in the reflectarray of the NASA MarCO mission [7].

The patch array feed allows for dynamically selecting one of two radiation patterns of the reflector according to the current acquisition modes by properly turning off and on some of the patch array elements.

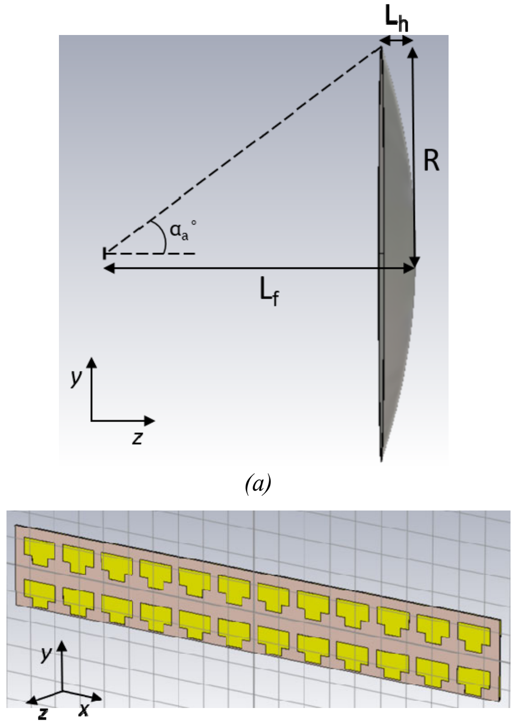

(a)

(b)

Figure 2: (a) Parabolic reflector. (b) 2x12 patch array feed.

4. SIMULATED PERFORMANCE

The antenna performances are calculated via a numerical EM solver based on a Finite-Difference Time-Domain method. In order to accelerate the simulation time and reduce the hardware requirements, the parabolic dish has been assumed of perfect electric conductor with 10 mesh cells per wavelength. Conversely, the patches and the ground plane have been assumed of copper.

The 2-dimensional radiation patterns are plotted in Figure 3 and Figure 4 for AM1 and AM2, respectively. Main performance parameters are listed in Table III and Table IV for AM1 and AM2, respectively.

The proposed antenna provides the required gain and HPBW in both AMs.

In AM1, the antenna offers high-gain performance for SNR improvement using only three nano-satellites as required by the formation definition. In the meantime, it ensures an adequate coverage of the area illuminated by the transmitter as the obtained HPBW is equal to 1.9 degree in both range and azimuth directions.

In AM2, the larger HPBW in the range direction allows for range swaths as large as 100 km, thus enabling monitoring of much wider areas.

The larger coverage area in AM2 is paid with a gain reduced by 6 dB with respect to AM1. The same loss is expected in NESZ and might be compensated by increasing the number of receiving satellites.

Finally, it is worth noting that this simulation study does not include some loss sources mainly related to the deployment mechanism, namely the surface ribs, struts, surface mesh, and surface accuracy. However, it is reasonable to assume such additional losses be less than 1 dB [6]. Therefore, they do not compromise the proper functioning of the antenna.

Table III: Antenna performance in AM1

Parameter	Value
Pointing (yz, xz)	(179.9, 180) deg
HPBW (yz, xz)	(1.9, 1.9) deg
Gain	37.5 dBi
SLL (yz, xz)	(-18.0, -16.0) dB
Edge taper (yz, xz)	(-5.75,-7) dB

Table IV: Antenna performance in AM2

Parameter	Value
Pointing (yz, xz)	(179.9, 180.0) deg
HPBW (yz, xz)	(1.8, 12.2) deg
Gain	31.4 dBi
SLL (yz, xz)	(-11.5, -29.5) dB
Edge taper (yz, xz)	(-5.56, -22.35) dB

5. CONCLUSION

In this paper we described the design of the receiving SAR antenna for a distributed FF-SAR operating at X-band and mounted onboard nano-satellites. The antenna was conceived to meet the requirements for two acquisition modes, namely a stripmap mode for SNR improvement and a HRWS imaging mode for wide-swath applications. The proposed receiving antenna consists of a large parabolic reflector illuminating a 2x12 patch array feed whose radiation pattern can be dynamically set according to the current acquisition mode.

Simulation results obtained with a numerical electromagnetic solver demonstrate that the proposed solution meets the requirements for both acquisition modes.

6. ACKNOWLEDGMENTS

This work has been supported by the Italian Ministry of University and Research through the project “FORmation flying of CubEsat assemblies for remote sensing (FORCE)”.

7. REFERENCES

[1] Nanosats database. Available from: www.nanosats.eu [Accessed: 07 January 2021].

[2] G. Di Martino, *et al.*, “Formation-Flying SAR Receivers in Far-from-Transmitter Geometry: Signal Model and Processing Scheme,” *IGARSS 2021 – 2021 IEEE Int. Geosci. Remote Sens. Symp.*, Brussels, July 2021.

[3] A. Moccia, A. Renga, Bistatic Synthetic Aperture Radar, in M. D’Errico (ed.) *Distributed Space Missions for Earth System Monitoring*, Space Technology Library, 2013, Vol. 31, Part 1, pp. 3-59, DOI: 10.1007/978-1-4614-4541-8_1.

[4] A. Renga, M. D. Graziano and A. Moccia, “Formation Flying SAR: analysis of imaging performance by Array Theory,” *IEEE Trans. Aerosp. Electron. Syst.*, doi: 10.1109/TAES.2020.3043526, 2020.

[5] V. Stanzione, B. Sabatinelli, “Platino Project: A new italian multi-application small satellite platform for highly competitive missions”, *69th International Astronautical Congress,* Bremen, Germany, 2018, 1–5 October.

[6] N. Chahat, *et al.*, “One-Meter Deployable Mesh Reflector for Deep-Space Network Telecommunication at X-Band and Ka-Band,” *IEEE Trans. Antennas Propag.*, vol. 68, no. 2, pp. 727-735, Feb. 2020.

[7] R. E. Hodges, *et al.*, "A Deployable High-Gain Antenna Bound for Mars: Developing a new folded-panel reflectarray for the first CubeSat mission to Mars.," *IEEE Antennas Propag. Mag.*, vol. 59, no. 2, pp. 39-49, April 2017.

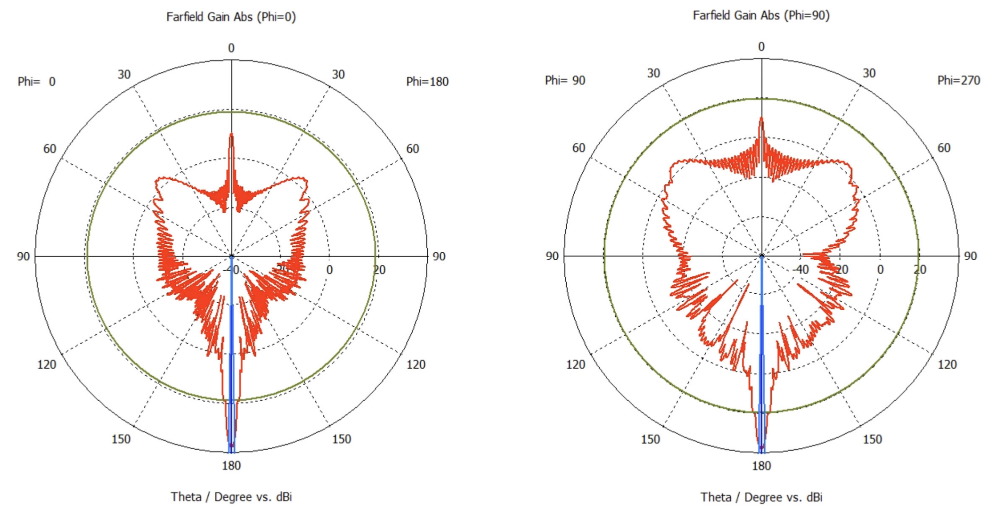

(a) *(b)*

Figure 3: Simulated radiation pattern at 9.6 GHz in AM1. (a) *xz* plane. (b) *yz* plane. Blue lines show the HPBW. Green circle represents sidelobe level (SLL).

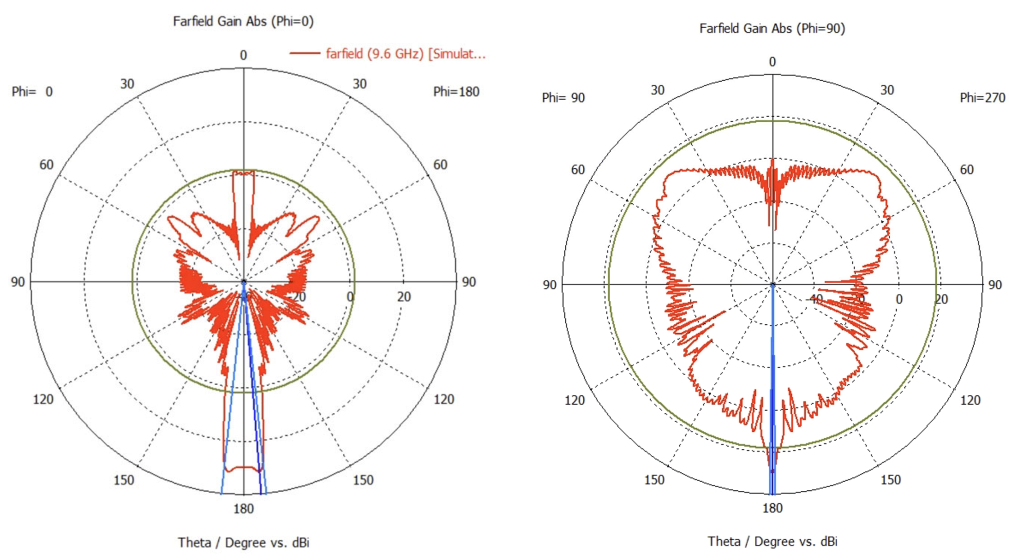

(a) *(b)*

Figure 4: Simulated radiation pattern at 9.6 GHz in AM2. (a) *xz* plane. (b) *yz* plane. Blue lines show the HPBW. Green circle represents sidelobe level (SLL).